Habenula volume increases with disease severity in unmedicated major depressive disorder as revealed by 7T MRI

Frank M. Schmidt, Stephanie Schindler, Melanie Adamidis, Maria Strauß, Anja Tränkner, Robert Trampel, Martin Walter, Ulrich Hegerl, et al.

European Archives of Psychiatry and Clinical Neuroscience

ISSN 0940-1334

Eur Arch Psychiatry Clin Neurosci
DOI 10.1007/s00406-016-0675-8

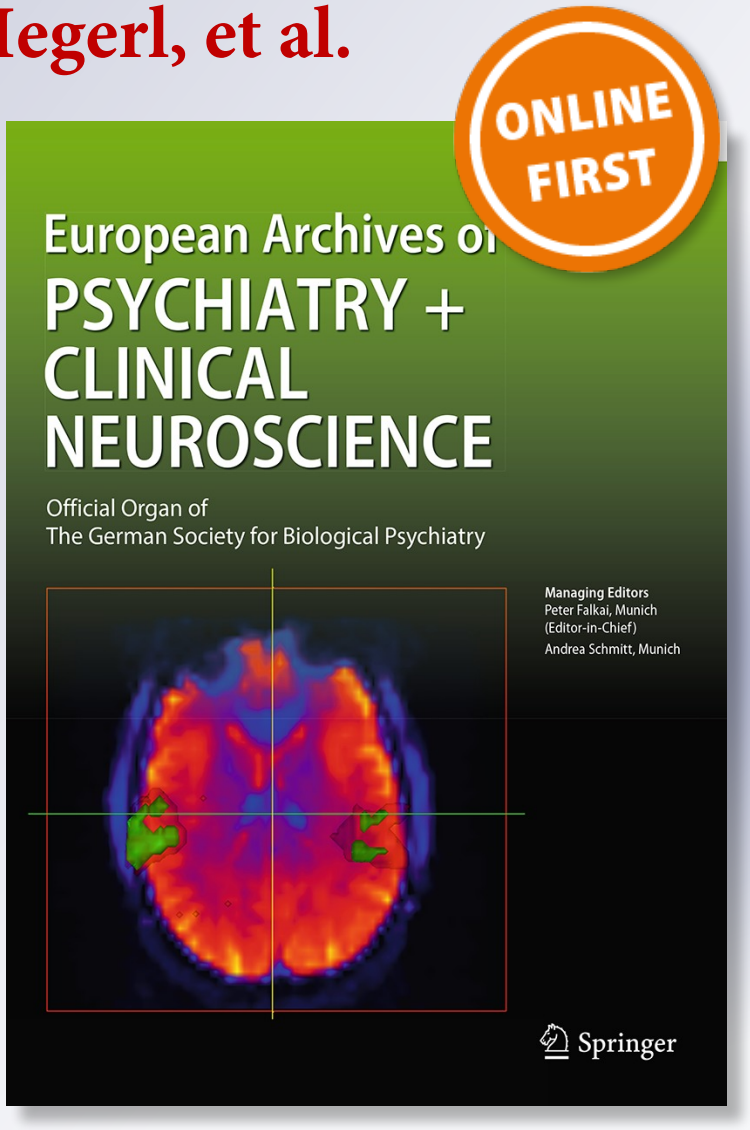

Springer

Eur Arch Psychiatry Clin Neurosci
DOI 10.1007/s00406-016-0675-8

ORIGINAL PAPER

Habenula volume increases with disease severity in unmedicated major depressive disorder as revealed by 7T MRI

Frank M. Schmidt[1] · Stephanie Schindler[1] · Melanie Adamidis[1] · Maria Strauß[1] · Anja Tränkner[1] · Robert Trampel[2] · Martin Walter[3] · Ulrich Hegerl[1] · Robert Turner[2] · Stefan Geyer[2] · Peter Schönknecht[1]

Received: 20 November 2015 / Accepted: 18 January 2016

Abstract The habenula is a paired epithalamic structure involved in the pathogenesis of major depressive disorder (MDD). Evidence comes from its impact on the regulation of serotonergic and dopaminergic neurons, the role in emotional processing and studies on animal models of depression. The present study investigated habenula volumes in 20 unmedicated and 20 medicated MDD patients and 20 healthy controls for the first time by applying a triplanar segmentation algorithm on 7 Tesla magnetic resonance (MR) whole-brain T1 maps. The hypothesis of a right-side decrease of habenula volumes in the MDD patients was tested, and the relationship between volumetric abnormalities and disease severity was exploratively investigated. Absolute and relative total and hemispheric habenula volumes did not differ significantly between the three groups. In the patients with short duration of disease for which medication effects could be ruled out, significant correlations were found between bilateral habenula volumes and HAMD-17- and BDI-II-related severities. In the medicated patients, this positive relationship disappeared. Our findings suggest an involvement of habenula pathology in the beginning of MDD, while general effects independent of severity or stage of disease did not occur. Our findings warrant future combined tractographic and functional investigation using ultra-high-resolution in vivo MR imaging.

Keywords 7 Tesla magnetic resonance imaging · Habenula · Major depression · MDD · MRI

Introduction

The habenula is a paired epithalamic structure with medial and lateral subdivisions which receive synaptic input predominantly from the lateral hypothalamus, amygdala and basal ganglia via the medullary stria, and project mainly to serotonergic dorsal (DRN) and medial (MRN) raphe nuclei, the dopaminergic ventral tegmental area (VTA), and the substantia nigra pars compacta [1]. Mainly inhibiting serotonergic and dopaminergic neuron activity [2], the habenula is regarded as a regulatory unit for the interplay between the cerebral cortex, limbic areas and monoaminergic activity of the midbrain [3]. Thus, it is involved in the adaptive response to stress, punishment and motor activity during reward processes [4–8]. In animal models of depression, lesions of the habenula led to a reduction of depressive behavior and to increased concentrations of serotonin (5-HT) in the DRN [9]. Habenula metabolism was increased in rats exhibiting depressive behavioral features which could be reversed by the application of antidepressants [10], potentially via the regulation of γ-aminobutyric acid [11]. In a mouse model of depression, the frequency of excitatory input of lateral habenula neurons onto VTA neurons was related to depressive behavior [10]. Pharmacological

Stefan Geyer and Peter Schönknecht shared senior authorship.

✉ Frank M. Schmidt
frank.schmidt2@medizin.uni-leipzig.de

Peter Schönknecht
peter.schoenknecht@medizin.uni-leipzig.de

[1] Clinic for Psychiatry and Psychotherapy, Department of Mental Health, University Hospital Leipzig, Semmelweisstr. 10, 04103 Leipzig, Germany

[2] Max Planck Institute for Cognitive and Brain Sciences, Stephanstr. 1a, 04103 Leipzig, Germany

[3] Clinical Affective Neuroimaging Laboratory, Leibniz Institute for Neurobiology, Otto-von-Guericke University, ZENIT building 65, Leipziger Str. 44, 39120 Magdeburg, Germany

Published online: 12 February 2016

inhibition and deep brain stimulation (DBS) of the habenula showed antidepressive effects in different rat models of depression [12–15]. Hence, according to the therapeutic response in major depressive disorder (MDD) [16], the habenular complex has become a proposed target site for DBS in MDD [17]. Investigations with positron emission tomography in unmedicated depressed patients showed that treatment response was predicted by pre-treatment serotonin transporter (SERT) binding ratios within the habenula [18]. A volumetric postmortem analysis in a mixed sample of 14 medicated unipolar and bipolar depressed patients (BP) [19] showed a reduction of right medial (−24 %) and lateral (−20 %) habenula volumes when compared to schizophrenic patients and controls. To date, two studies have investigated habenula volumes in MDD patients in vivo [20–22]. Using 3-Tesla magnetic resonance (MR) images, the first investigation revealed decreased right hemisphere habenula volumes in female MDD patients. Smaller absolute and relative habenula left and right volumes were found in BP compared to controls. In contrast, the recent analysis showed that medicated women with a first-episode MDD had higher overall habenula volumes compared to healthy controls [22]. When investigating patients with post-traumatic stress disorder, significant volume differences compared to controls were not found [23].

The cellular correlates of habenula volume changes in mood disorders have been largely unknown. Recent evidence converges on cell-type-specific trajectories which distinguish early, mainly astroglial involvement [15] followed by chronic neuronal damage and even glial swelling during the later course of the disease [24]. To better understand pathological changes, first or recurrent disease episode as well as psychotropic medication has to be taken into account. But most important, given the small size of this structure, an increase in spatial resolution by using recent ultra-high field methods is essential [25].

In the present study, we investigated habenula volumes in 20 unmedicated and 20 medicated acutely ill MDD patients and 20 healthy controls by applying a triplanar segmentation algorithm to 7T MR images. Based on prior findings, a right-side decrease of habenula volumes was expected in the MDD patients. Furthermore, since little evidence exists to which extent volumetric abnormalities do correlate with disease severity, we investigated exploratively this relationship in both patient samples.

Methods

Subjects

Patients meeting the criteria of the Diagnostic Statistical Manual IV (DSM IV) for a depressive episode or recurrent depressive disorder were recruited from the Department of Mental Health, Clinic for Psychiatry and Psychotherapy, University Hospital Leipzig. Disease severity, confirmation of diagnosis, and psychiatric comorbidities were assessed using a structured clinical interview for DSM IV (SCID) under supervision of a specialist in psychiatry. Disease severity at the time of scanning was quantified using the Hamilton Depression Rating Scale (HAMD-17), Inventory of Depressive Symptoms (IDS-C), Beck Depression Inventory II (BDI-II), and Bech Rafaelsen Melancholia Scale (BRMS). Exclusion criteria were: history or incidental findings of neurological disorders, history of head injury >*I*°, suicidality, current or earlier substance abuse or addiction, severe somatic disorder, and general MR imaging exclusion criteria. For the healthy controls, exclusion criteria further comprised a lifetime history of psychiatric diagnoses. All subjects gave written informed consent. The study protocol was approved by the Ethics Committee of the University of Leipzig.

Image acquisition

Whole-brain T1-maps images were acquired with a 7T whole-body MR scanner (MAGNETOM 7T, Siemens, Erlangen, Germany) and a 24-channel NOVA head coil (Nova Medical, Inc., Wilmington MA, USA). A modified 3D magnetization-prepared 2 rapid acquisition gradient echoes sequence (3D MP2RAGE [26]) was used with repetition time (TR) = 8250 ms, inversion times (TI1/TI2) = 1000/3300 ms, flip angles (FA1/FA2) = 7°/5°, echo time (TE) = 2.51 ms, bandwidth (BW) = 240 Hz/Pixel, 1 average. A field of view (FOV) of 224 × 224 mm^2, an imaging matrix of 320 × 320, and 240 slices with a thickness of 0.7 mm resulted in a nominal acquisition voxel size of 0.7 mm isotropic. By accelerating the acquisition using parallel imaging (GRAPPA [27]; acceleration factor = 2), a scan time of 18:02 min was achieved. The whole-brain volume (WBV) was determined using FMRIB Software Library (FSL) [28] using native brain images after skull-stripping with Medical Image Processing, Analysis, and Visualization (MIPAV) version 6.0.0 [29].

Computer-assisted interactive segmentation of the habenula on 7T MR images

The interactive habenula segmentation in triplanar view was performed using ITK-SNAP [30] version 2.2.0. In order to assure constant contrast in all images, a fixed intensity scale was used ranging from $I = 0$ (black) to $I = 4000$ (white). First, habenula landmarks were developed with reference to the postmortem single brain atlas by Mai et al. [31]. Based on the landmarks, a detailed interactive segmentation algorithm of the habenula on high-resolution

Table 1 Interactive segmentation algorithm of the habenula

Anterior	Posterior	Medial	Lateral	Superior	Inferior
Segmentation landmarks in coronal planes					
Disbandment of cohesive nuclei (<3 voxel width) and transition to medullary stria	Last voxel with a identifiable paired structure, anterior to pineal recess/pineal gland one voxel more posterior if clearly related in both transversal and sagittal planes	Cerebrospinal fluid	Thalamus	Cerebrospinal fluid (more posterior) thalamus (more anterior)	Posterior commissure (more posterior) thalamus (more anterior)
Conservative decision	Conservative decision	Liberal decision	Conservative decision	Liberal decision	Conservative decision
Segmentation landmarks in transversal planes					
Proof of plausibility in coronal and transversal sections					
Medullary stria	Posterior commissure pineal recess cerebrospinal fluid	Cerebrospinal fluid	Thalamus	Thalamus	Posterior commissure pineal recess
Conservative decision	Conservative decision	Liberal decision	Conservative decision	Conservative decision	Conservative decision
Segmentation landmarks in sagittal planes					
Proof of plausibility in coronal and transversal sections					
Thalamus medullary stria	Pineal recess	Cerebrospinal fluid	Thalamus	Thalamus	Thalamus
Conservative decision	Conservative decision	Liberal decision	Conservative decision	Conservative decision	Conservative decision

T1 maps was developed (Table 1; Fig. 1). The region of interest (ROI) included the entire habenula complex (i.e., medial and lateral division) in both hemispheres. The medullary stria, fasciculus retroflexus, and habenular commissure were excluded from segmentation. The habenula was segmented unilaterally in all three planes. The first segmentation step was performed in coronal planes which served as reference. This means that the segmentation results in the other two planes (transverse, second step, and sagittal, third step) were rechecked in the coronal plane, and voxels were added or rejected in these planes according to the anatomical plausibility in the coronal plane. Depending on the border of the habenula, each rater was trained to include (liberal decision) or to exclude (conservative decision) inconclusive voxel (Table 1). We determined a cutoff value in each landmark which was applied in anatomically inconclusive voxels. Accordingly, voxel with gray level intensity >1800 was attributed to non-habenular tissue and with gray level intensity >3000 to surrounding cerebrospinal fluid. Projections which deviated from the outline of the mask to the maximum length of one voxel were reduced. After a training period, two investigators (F.S., M.A.) traced the left and the right habenula of ten subjects in independent segmentation runs. The inter-rater reliability (ICC; [32]) was 0.95 for the right and 0.96 for the left habenula. During all segmentations, raters were blind to diagnosis.

Statistics

Following normal distribution of habenula volumes (Kolmogorov–Smirnov test: $p > 0.05$), the hypothesis of reduced right-side habenula in MDD was tested by applying a general linear model with repeated measures with absolute and relative right-versus-left hemisphere as within-subjects factor and group, sex, and the interaction of group and sex as the between-subjects factors. For absolute and relative bihemispheric habenula volumes, ANOVA with volume as the dependent variable and group and sex as the categorical independent variables was applied. For differences of WBV between groups, single-factor ANOVA was applied. For differences between groups regarding sex and handedness, Chi-square tests were computed. For differences in sum scores of BDI-II, HAMD-17, IDS-C and BRMS, Mann–Whitney *U* tests were applied. Group differences regarding age and number of depressive episodes were tested with independent samples *t* tests. A median-split of the HAMD-17 scores resulted in a cutoff of 17 points separating mildly from moderate-to-severely depressed patients. Correlations between habenula volumes and clinical variables were performed with Spearman's rank correlation coefficient. For post hoc analyses of individual group differences in habenula volume, single-factor

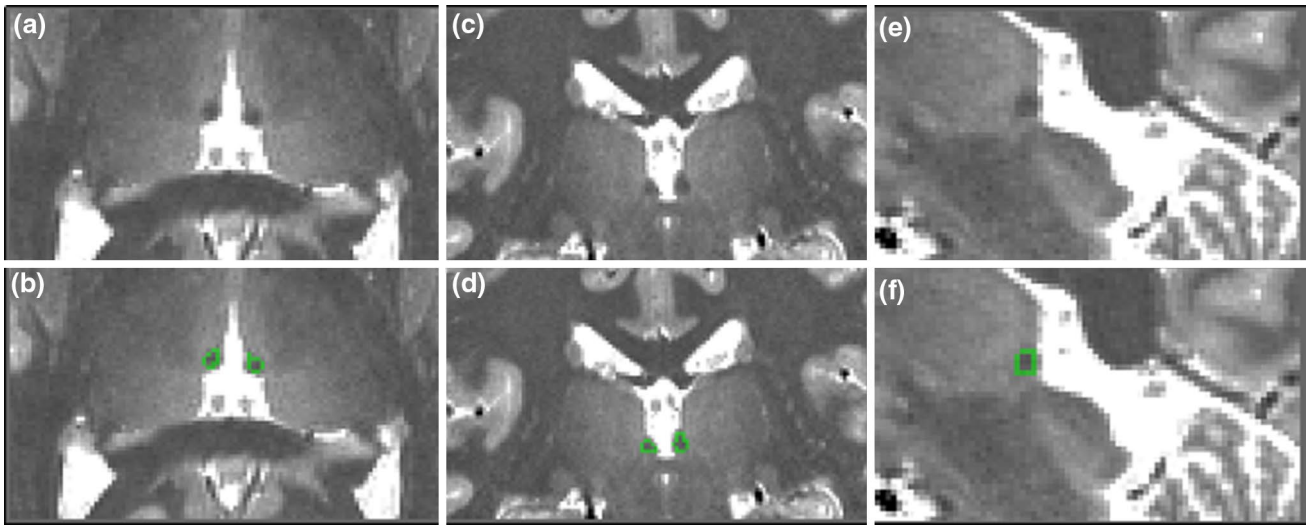

Fig. 1 Habenula nuclei in the coronal (**a**, **b**) transversal (**c**, **d**), and sagittal (**e**, **f**) planes. Native T1 maps (**a**, **c**, **e**) and T1 maps with segmented habenula voxels overlay in *green* (**b**, **d**, **f**). For segmentation algorithm, see Table 1

ANOVAs and independent samples *t* test were applied. For all analyses, level for significance was set at $p < 0.05$.

Results

Groups did not vary in clinical variables age, sex, and handedness, whereas unmedicated depressed patients had significantly fewer episodes of depression compared to medicated patients (Table 2).

No interactions between the within-subjects factor 'hemisphere' and between-subjects factor 'group' were observed in absolute ($F = 1.776$, $p = 0.179$) and relative habenula volumes ($F = 0.000$, $p = 1.00$; Table 2; Fig. 2a). Interaction analyses for 'hemisphere × sex' revealed significance for relative volumes ($F = 7.789$, $p = 0.007$) but not absolute volumes ($F = 0.138$, $p = 0.712$). Post hoc tests between sexes on relative volumes revealed a difference of 13 % in right (males right: $1.05 \times 10^{-5} \pm 2.53 \times 10^{-6}$ mm^3; females right: $1.21 \times 10^{-5} \pm 2.53 \times 10^{-6}$ mm^3; $F = 2.663$, $p = 0.054$) and 12 % in left relative habenula (males left: $1.03 \times 10^{-5} \pm 2.50 \times 10^{-6}$ mm^3; left: $1.16 \times 10^{-5} \pm 2.50 \times 10^{-6}$, left $F = 2.265$, $p = 0.096$). No interactions between 'hemisphere × groups × sex' were found for absolute volumes ($F = 0.096$, $p = 0.909$) nor relative volumes ($F = 0.000$, $p = 1.000$).

No significant differences in total absolute and total relative habenula volumes were observed between the three groups (Table 2). Interaction between volumes × sex trended in the relative habenula volumes ($F = 3.059$, $p = 0.086$; absolute volumes: $F = 0.097$, $p = 0.757$). No significant interaction between total volumes × groups × sex arose (absolute volumes: $F = 0.096$, $p = 0.909$; relative volumes: $F = 0.000$, $p = 1.000$).

Variances for total and hemispheric habenula volumes were found significantly lower in the medicated MDD when compared to the unmedicated MDD and healthy controls (3-group comparison: total volume absolute: $p = 0.004$, relative: $p = 0.01$, right hemisphere volume absolute: $p = 0.037$, relative: $p = 0.031$, left hemisphere volume absolute: $p = 0.011$, relative: $p = 0.108$; see Fig. 2). In these cases of unequal variances, ANOVA tends to be liberal [33], i.e., the true alpha error might exceed the *p* value reported here. However, according to [34], the requirements for a robust ANOVA with heterogeneous variances are fulfilled, as the number of subjects in each group is similar, the populations are normally distributed, and the ratio of the largest variance/smallest variance is <=3.

Correlation analyses between habenula volumes and severity of depressive episodes in the unmedicated MDD showed significant correlations between HAMD-17 scores and absolute right, absolute left, relative left, and absolute bihemispheric habenula volumes. For BDI-II and IDS-C, significant correlations were found for the absolute left habenula volume. Nonsignificant trends were found for correlations between the HAMD-17 and the relative bihemispheric volume, between the BDI-II and relative left and absolute bihemispheric volumes and between the IDS-C and absolute bihemispheric habenula volumes. For the medicated MDD, none of the severity scores were found to correlate with habenula volumes (Table 3; Fig. 2b). Divided

Table 2 Clinical characteristics and habenula volumes

	Unmed. MDD ($n = 20$)	Med. MDD ($n = 20$)	HC ($n = 20$)	Test statistic	p values
Age at scan (years ± SD)[a]	36.20 ± 12.83	40.60 ± 12.11	36.45 ± 13.16	$F = 0.757$	0.474
Sex (female/male)[b]	12/8	13/7	12/8	$\chi^2 = 0.141$	0.932
Hand (right/left)[b]	19/1	19/1	18/2	$\chi^2 = 0.536$	0.765
HAMD-21 (score ± SD)[c]	16.40 ± 7.76	15.55 ± 8.89	NA	$F = 0.992$	0.749
BDI-II (score ± SD)[c]	26.35 ± 10.19	21.60 ± 10.59	NA	$F = 0.062$	0.157
IDS-C (score ± SD)[c]	31.30 ± 12.35	29.40 ± 13.00	NA	$F = 0.011$	0.638
BRMS (score ± SD)[c]	16.30 ± 4.94	14.40 ± 7.39	NA	$F = 4.357$	0.345
Number of depressive episodes (±SD)[d]	1.70 ± 1.56	5.75 ± 5.47	NA	$F = 6.995$	0.003
Absolute total Hb volume (in mm^3 ± SD)[a]	34.99 ± 12.04	34.16 ± 3.52	34.92 ± 11.34	$F = 0.045$	0.956
Relative total Hb volume[a]	$2.23 \times 10^{-5} \pm 6.73 \times 10^{-6}$	$2.25 \times 10^{-5} \pm 3.07 \times 10^{-6}$	$2.26 \times 10^{-5} \pm 7.68 \times 10^{-6}$	$F = 0.000$	1.000
Absolute right Hb volume (in mm^3 ± SD)[a]	17.80 ± 6.41	17.70 ± 2.78	17.29 ± 6.12	$F = 0.051$	0.950
Relative right Hb volume[a]	$1.15 \times 10^{-5} \pm 3.67 \times 10^{-6}$	$1.17 \times 10^{-5} \pm 2.06 \times 10^{-6}$	$1.12 \times 10^{-5} \pm 4.19 \times 10^{-6}$	$F = 0.000$	1.000
Absolute left Hb volume (mm^3 ± SD)[a]	17.18 ± 5.94	16.45 ± 2.49	17.63 ± 5.49	$F = 0.295$	0.746
Relative left Hb volume[a]	$1.11 \times 10^{-5} \pm 3.32 \times 10^{-6}$	$1.09 \times 10^{-5} \pm 2.01 \times 10^{-6}$	$1.14 \times 10^{-5} \pm 3.62 \times 10^{-6}$	$F = 0.000$	1.000
WBV (mm^3 ± SD)[a]	1,543,088 ± 159,754	1,529,104 ± 140,602	1,554,703 ± 122,644	$F = 1.164$	0.331

Hb habenula, *HAMD* Hamilton Depression Rating Scale, *BDI-II* Beck Depression Inventory, *IDS-C* Inventory of Depressive Symptoms, *BRMS* Bech Rafaelsen Melancholia Scale, *SD* standard deviation, *WBV* whole-brain volume

[a] Single-factor ANOVA

[b] Chi-square test

[c] Mann–Whitney *U* tests

[d] Independent samples *t* test

into groups according to the severity of depression in the HAMD-17 scores at time of scan, the unmedicated moderate-to-severely depressed MDD ($n = 10$) showed significantly higher absolute left (20.07 ± 6.38 mm^3; $p = 0.026$) and absolute bihemispheric habenula volumes (40.44 ± 13.19 mm^3; $p = 0.039$) compared to the unmedicated mildly depressed MDD (absolute left volume 15.23 ± 4.67 mm^3; absolute bihemispheric volume 29.54 ± 8.14 mm^3; $n = 10$). Between these groups, mean differences in relative left (moderate–severe $0.97 \times 10^{-5} \pm 2.64 \times 10^{-6}$ mm^3, mild $1.25 \times 10^{-5} \pm 3.47 \times 10^{-6}$ mm^3; $p = 0.061$) and absolute right volumes (moderate–severe 20.37 ± 7.09 mm^3, mild 15.23 ± 4.67 mm^3; $p = 0.072$) showed a trend toward significance. For the medicated MDD, no significant difference in volumes between the mildly depressed ($n = 9$) and moderate-to-severely depressed patients ($n = 11$) arose.

No significant correlations were found between relative and absolute habenula volumes and age within the overall sample as well the separate groups.

Discussion

To our knowledge, this is the first high-resolution 7T MR-based three-dimensional volumetric investigation of habenula volumes in human subjects applied in a sample of unmedicated MDD patients, medicated MDD patients, and healthy controls.

In accordance with the two in vivo MR imaging (3T) studies in MDD published to date [20–22], the bihemispheric habenula volume did not differ between unmedicated or medicated MDD compared to controls. In addition, by exploiting the potential of the high magnetic field strength to reveal small alterations in cerebral morphology, we did not find hemispheric or sex-related differences in habenula volume change in MDD patients. However, we could demonstrate significant correlations between habenula volume and disease severity in unmedicated MDD, but not in medicated patients. We found a significant habenula volume increase in severely compared to mildly depressed unmedicated patients, whereas no such volume differences existed in the medicated group.

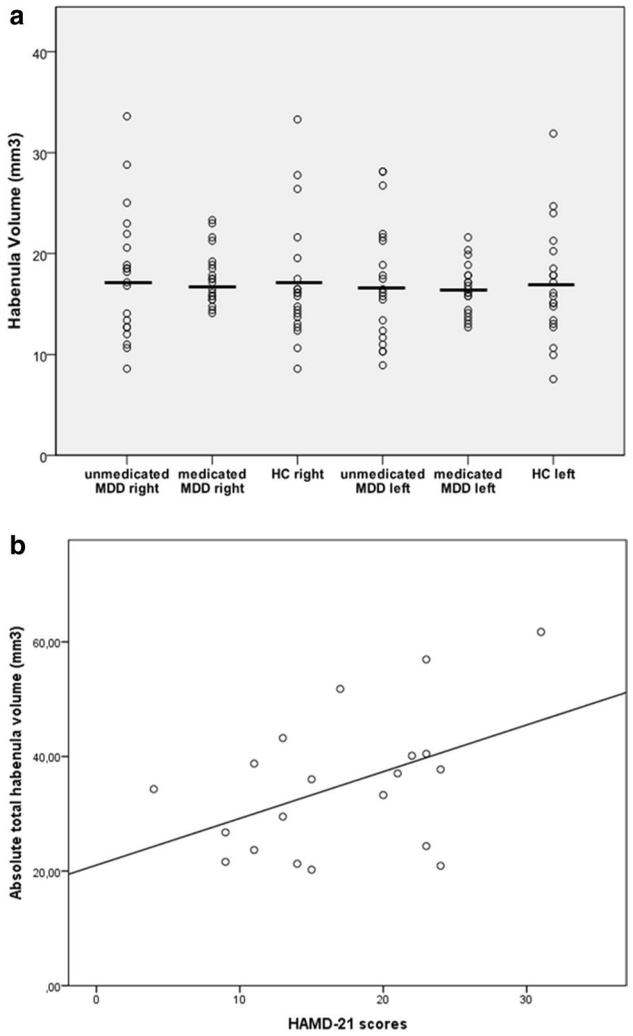

Fig. 2 **a** Scatterplot of absolute hemispheric habenula volumes across the diagnostic groups. Means did not differ significantly between groups, whereas variances were found reduced in the medicated MDD. *MDD* major depressive disorder, *HC* healthy controls. **b** Significant correlation between total scores in HAMD-21 and absolute habenula volumes in the unmedicated MDD ($r = 0.508$, $p < 0.05$)

These findings as well as a markedly reduced variation in habenula volumes in the medicated group point toward a potential effect of medication or stage of disease on habenula volume. Concerning an influence of duration of the disorder, support comes from a recent study showing volume differences between medicated females only in those patients with a first-time episode as well as moderate negative correlations between habenula volumes and disease duration [22]. A state-dependent volume change which should hold true only during an acute episode may be assumed. Although habenula volumes did not correlate with the number of episodes within this study, the fact of significantly fewer depressive episodes in unmedicated compared to medicated patients further supports that changes in habenula volumes may be restricted to the early course of the disorder. Furthermore, in the unmedicated patients, the backward inhibition from serotonergic and dopaminergic regions [1] may be reduced. In the medicated subjects, the antidepressant medication may compensate for the pathogenic reduction in inhibition, as seen in animal models of depression [10, 11, 15].

The importance of disease stage on glial and neuronal development has recently been stressed by Rajkowska and Miguel-Hidalgo [24]. They argued for primary reductions in glial numbers within the beginning of the disorder, leaving neuronal cells unaffected; at later stages, chronic excitotoxicity would lead to neuronal decline and astroglial swelling. Acknowledging variations to these cortical processes, increases in both gliogenesis and neurogenesis may be found, especially in subcortical structures that could lead to opposite volumetric effects. Such a model favors our findings showing increased volumes, especially in acutely and severely depressed patients with a clinical course of one or only a few episodes. Taking into consideration that clinical severity itself may be a risk factor for chronification [35], it is striking to see that most severe cases show early volume increases followed by a gradual decrease toward uniformly low volumes at a chronic stage. In other words, one may expect our medicated chronic group to be more homogeneous than the unmedicated sample which would be reflected by the smaller variations in habenula volumes.

One of the strengths of the present study—in contrast to reliable but only approximate geometric approaches [36]—is its methodologically approach based on a three-dimensional segmentation algorithm in coronal, transversal and sagittal planes of high-resolution 7T MR images. This provides the basis for a reliable identification of the habenula and the precise definition of borders to surrounding anatomical structures. Furthermore, the quantitative T1 maps show a strong contrast between the habenula and surrounding brain tissue due to the high myelin content of the habenula as a white matter structure connecting limbic and midbrain areas [37, 38]. There is very strong evidence that maps of T1 values reflect cortical myelin content [39], which encourages the use of such maps for cortical parcellation based on myelination at high field strengths [37]. Conventional T1-weighted images are, however, not only sensitive to differences in T1 relaxation but also to other factors, like proton density or T2*, depending on the sequence parameters used. Since T1-weighted images as applied in the aforementioned study [20] do not specifically reflect myelin content, the different display of the two studies may further account for the differing results.

A calculation of the interaction between sexes and hemisphere showed, irrespective of the group, a 12–13 %

Table 3 Association between clinical variables and habenula volumes

	Absolute right Hb volume	Relative right Hb volume	Absolute left Hb volume	Relative left Hb volume	Absolute total Hb volume	Relative total Hb volume
Unmedicated MDD						
Age at scan	$r = -0.061$, $p = 0.799$	$r = 0.039$, $p = 0.871$	$r = -0.013$, $p = 0.956$	$r = 0.080$, $p = 0.737$	$r = -0.226$, $p = 0.339$	$r = 0.061$, $p = 0.799$
Number of episodes	$r = -0.021$, $p = 0.929$	$r = -0.052$, $p = 0.830$	$r = -0.002$, $p = 0.993$	$r = -0.027$, $p = 0.909$	$r = 0.149$, $p = 0.530$	$r = -0.041$, $r = 0.862$
BDI-II	$r = 0.359$, $p = 0.120$	$r = 0.274$, $p = 0.243$	**$r = 0.462$, $p = 0.040$**	$r = 0.415$, $p = 0.069$	$r = 0.419$, $p = 0.066$	$r = 0.354$, $p = 0.126$
HAMD-21	**$r = 0.474$, $p = 0.035$**	$r = 0.371$, $p = 0.107$	**$r = 0.519$, $p = 0.019$**	**$r = 0.457$, $p = 0.043$**	**$r = 0.508$, $p = 0.022$**	$r = 0.428$, $p = 0.060$
IDS-C	$r = 0.370$, $p = 0.108$	$r = 0.227$, $p = 0.336$	**$r = 0.459$, $p = 0.042$**	$r = 0.364$, $p = 0.114$	$r = 0.424$, $p = 0.063$	$r = 0.304$, $p = 0.193$
BRMS	$r = 0.368$, $p = 0.111$	$r = 0.317$, $p = 0.174$	$r = 0.370$, $p = 0.109$	$r = 0.346$, $p = 0.135$	$r = 0.378$, $p = 0.100$	$r = 0.343$, $p = 0.138$
Medicated MDD						
Age at scan	$r = -0.126$, $p = 0.598$	$r = -0.044$, $p = 0.853$	$r = -0.294$, $p = 0.208$	$r = -0.169$, $p = 0.477$	$r = -0.129$, $p = 0.589$	$r = -0.140$, $p = 0.556$
Number of episodes	$r = -0.206$, $p = 0.398$	$r = 0.039$, $p = 0.874$	$r = 0.076$, $p = 0.758$	$r = 0.348$, $p = 0.144$	$r = -0.372$, $p = 0.117$	$r = 0.356$, $p = 0.135$
BDI-II	$r = -0.295$, $p = 0.208$	$r = -0.250$, $r = 0.287$	$r = -0.007$, $p = 0.976$	$r = 0.057$, $p = 0.812$	$r = -0.009$, $p = 0.969$	$r = -0.130$, $p = 0.584$
HAMD-21	$r = -0.097$, $p = 0.683$	$r = -0.204$, $p = 0.387$	$r = -0.116$, $p = 0.627$	$r = -0.158$, $p = 0.505$	$r = 0.221$, $p = 0.349$	$r = -0.240$, $p = 0.308$
IDS-C	$r = -0.210$, $p = 0.373$	$r = -0.241$, $p = 0.305$	$r = 0.044$, $p = 0.853$	$r = 0.029$, $p = 0.902$	$r = -0.135$, $p = 0.571$	$r = -0.142$, $p = 0.549$
BRMS	$r = -0.099$, $p = 0.678$	$r = -0.167$, $p = 0.481$	$r = -0.071$, $p = 0.765$	$r = -0.096$, $p = 0.688$	$r = -0.129$, $p = 0.589$	$r = -0.174$, $p = 0.462$
HC						
Age at scan	$r = -0.058$, $p = 0.808$	$r = 0.017$, $p = 0.943$	$r = -0.161$, $p = 0.498$	$r = -0.081$, $p = 0.735$	$r = -0.109$, $p = 0.647$	$r = -0.029$, $p = 0.904$

Significant correlations are in bold

BDI-II Beck Depression Inventory, *HAMD* Hamilton Depression Rating Scale, *IDS-C* Inventory of Depressive Symptoms, *BRMS* Bech Rafaelsen Melancholia Scale, *HC* healthy controls

reduction in mean volumes in males compared to females. Support for a potential sexual dimorphism in habenula volumes comes from studies that detected sex hormone-binding globulin [40] and estrogen receptors [41] in the habenula that facilitate female sexual receptivity [42]. Given the strong glutamatergic input to the habenula, the previously discussed neuroprotective mechanisms of estrogen receptors such as upregulation of glutamine synthetase and glutamate transporters [43] would support our observation and further strengthen the role of glial mechanisms in regulating habenula size. Furthermore, the habenula contains progesterone-sensitive arginine vasopressin-immunoreactive fibers originating from neurons in the amygdala which are known to be higher in number in males and to influence anxiety-related behavior, social affiliation, and aggression [44]. Also, cytochrome oxidase activity as an indicator of cerebral metabolic capacity was found elevated in the female compared to male habenula [45]. Though an interaction between habenula volume and sex independent of a diagnosis of MDD has not been investigated in the two structural studies [19, 20], the finding of reduced habenula volumes in female MDD patients prompted the authors [20] to argue that excitotoxic damage to the habenula is more pronounced in females than in males.

The present study has several limitations that need to be addressed. The size of the present sample and subgroups may have led to type II errors with an under-recognition of possible subtle differences in habenula volumes between groups. We have to acknowledge that by using the present approach, even on high-resolution 7T MR, it was not possible to separate the habenula into medial and lateral divisions as it has been shown ex vivo [25]. Since both components appear to have some independent functions, the combined measurement may not therefore fully account for distinct changes in

habenula volumes. Therefore, we are cautious interpreting data on separated white and gray matter of the habenula in 3T-images [22]. Thirdly, a shift of diagnosis during the clinical course, e.g., to a disorder of the bipolar spectrum, especially in those patients with first-time depression included in the study, is to be expected according to the literature, with a concomitant impact on habenula volumes. Long-term follow-up investigations are therefore recommended [46].

In conclusion, this is the first ultra-high-resolution 7T MR-based volumetric investigation of the human habenula which showed a significant correlation between habenula volume and disease severity in unmedicated MDD patients and an increase in habenula volume in moderate-to-severely depressed unmedicated (but not medicated) MDD patients compared to mildly depressed patients, respectively. Evidence is given for a general sex effect across all groups, whereas lateralized volume reductions only in females as reported at lower MR field strengths could not be replicated.

Acknowledgments We thank Dr. R. Mergl for technical assistance in analyzing the data.

Conflict of interest All authors declare no conflict of interests.

References

1. Hikosaka O (2010) The habenula: from stress evasion to value-based decision-making. Nat Rev Neurosci 11:503–513
2. Brinschwitz K, Dittgen A, Madai VI, Lommel R, Geisler S, Veh RW (2010) Glutamatergic axons from the lateral habenula mainly terminate on GABAergic neurons of the ventral midbrain. Neurosci 168:463–476
3. Poller WC, Bernard R, Derst C, Weiss T, Madai VI, Veh RW (2011) Lateral habenular neurons projecting to reward-processing monoaminergic nuclei express hyperpolarization-activated cyclic nucleotid-gated cation channels. Neurosci 193:205–216
4. Ide JS, Li CS (2011) Error-related functional connectivity of the habenula in humans. Front Hum Neurosci 5:25
5. Amat J, Sparks PD, Matus-Amat P, Griggs J, Watkins LR, Maier SF (2001) The role of the habenular complex in the elevation of dorsal raphe nucleus serotonin and the changes in the behavioral responses produced by uncontrollable stress. Brain Res 917:118–126
6. Matsumoto M, Hikosaka O (2007) Lateral habenula as a source of negative reward signals in dopamine neurons. Nature 447:1111–1115
7. Matsumoto M, Hikosaka O (2009) Representation of negative motivational value in the primate lateral habenula. Nat Neurosci 12:77–84
8. Zhao H, Zhang BL, Yang SJ, Rusak B (2015) The role of lateral habenula-dorsal raphe nucleus circuits in higher brain functions and psychiatric illness. Behav Brain Res 277:89–98
9. Yang LM, Hu B, Xia YH, Zhang BL, Zhao H (2008) Lateral habenula lesions improve the behavioral response in depressed rats via increasing the serotonin level in dorsal raphe nucleus. Behav Brain Res 188:84–90
10. Caldecott-Hazard S, Mazziotta J, Phelps M (1988) Cerebral correlates of depressed behavior in rats, visualized using 14C-2-deoxyglucose autoradiography. J Neurosci 8:1951–1961
11. Shabel SJ, Proulx CD, Piriz J, Malinow R (2014) Mood regulation. GABA/glutamate co-release controls habenula output and is modified by antidepressant treatment. Science 345:1494–1498
12. Li B, Piriz J, Mirrione M, Chung C, Proulx CD, Schulz D, Henn F, Malinow R (2011) Synaptic potentiation onto habenula neurons in the learned helplessness model of depression. Nature 470:535–539
13. Meng H, Wang Y, Huang M, Lin W, Wang S, Zhang B (2011) Chronic deep brain stimulation of the lateral habenula nucleus in a rat model of depression. Brain Res 1422:32–38
14. Winter C, Vollmayr B, Djodari-Irani A, Klein J, Sartorius A (2011) Pharmacological inhibition of the lateral habenula improves depressive-like behavior in an animal model of treatment resistant depression. Behav Brain Res 216:463–465
15. Cui W, Mizukami H, Yanagisawa M, Aida T, Nomura M, Isomura Y, Takayanagi R, Ozawa K, Tanaka K, Aizawa H (2014) Glial dysfunction in the mouse habenula causes depressive-like behaviors and sleep disturbance. J Neurosci 34:16273–16285
16. Sartorius A, Kiening KL, Kirsch P, von Gall CC, Haberkorn U, Unterberg AW, Henn FA, Meyer-Lindenberg A (2010) Remission of major depression under deep brain stimulation of the lateral habenula in a therapy-refractory patient. Biol Psychiatry 67:e9–e11
17. Kiening K, Sartorius A (2013) A new translational target for deep brain stimulation to treat depression. EMBO Mol Med 5:1151–1153
18. Lanzenberger R, Kranz GS, Haeusler D, Akimova E, Savli M, Hahn A, Mitterhauser M, Spindelegger C, Philippe C, Fink M, Wadsak W, Karanikas G, Kasper S (2012) Prediction of SSRI treatment response in major depression based on serotonin transporter interplay between median raphe nucleus and projection areas. Neuroimage 63:874–881
19. Ranft K, Dobrowolny H, Krell D, Bielau H, Bogerts B, Bernstein HG (2010) Evidence for structural abnormalities of the human habenular complex in affective disorders but not in schizophrenia. Psychol Med 40:557–567
20. Savitz JB, Nugent AC, Bogers W, Vythilingam M, Bogers W, Charney DS, Drevets WC (2011) Habenula volume in bipolar disorder and major depressive disorder: a high-resolution magnetic resonance imaging study. Biol Psychiatry 69:336–343
21. Savitz JB, Rauch SL, Drevets WC (2013) Reproduced from Habenula volume in bipolar disorder and major depressive disorder: a high-resolution magnetic resonance imaging study. Mol Psychiatry 18:523
22. Carceller-Sindreu M, de Diego-Adeliño J, Serra-Blasco M, Vives-Gilabert Y, Martí N-Blanco A, Puigdemont D, Álvarez E, Pérez V, Portella MJ (2015) Volumetric MRI study of the habenula in first episode, recurrent and chronic major depression. Eur Neuropsychopharmacol. doi:10.1016/j.euroneuro.2015.08.009
23. Savitz JB, Bonne O, Nugent AC, Vythilingam M, Bogers W, Charney DS, Drevets WC (2011) Hanenula volume in post-traumatic stress disorder measured with high-resolution MRI. Biol Mood Anxiety Disord 1:7
24. Rajkowska G, Miguel-Hidalgo JJ (2007) Gliogenesis and glial pathology in depression. CNS Neurol Disord: Drug Targets 6:219–233
25. Strotmann B, Heidemann RM, Anwander A, Weiss M, Trampel R, Villringer A, Turner R (2014) High-resolution MRI and diffusion-weighted imaging of the human habenula at 7 Tesla. J Magn Reson Imaging 39:1018–1026
26. Marques JP, Kober T, Krueger G, van der Zwaag W, Van de Moortele PF, Gruetter R (2010) MP2RAGE, a self bias-field corrected sequence for improved segmentation and T1-mapping at high field. Neuroimage 49:1271–1281

27. Griswold MA, Jakob PM, Heidemann RM, Nittka M, Jellus V, Wang J, Kiefer B, Haase A (2002) Generalized Autocalibrating Partially Parallel Acquisitions (GRAPPA). Magn Reson Med 47:1202–1210
28. Jenkinson M, Beckmann CF, Behrens TE, Woolrich MW, Smith SMFSL (2012) Neuroimage 62:782–790
29. Bazin PL, Cuzzocreo JL, Yassa MA, Gandler W, McAuliffe MJ, Bassett SS, Pham DL (2007) Volumetric neuroimage analysis extensions for the MIPAV software package. J Neurosci Methods 165:111–121
30. Yushkevich PA, Piven J, Hazlett HC, Ho S, Gee JC, Gerig G (2006) User-guided 3D active contour segmentation of anatomical structures: significantly improved efficiency and reliability. Neuroimage 31:1116–1128
31. Mai JK, Paxinos G, Voß T (2008) Atlas of the human brain. Academic Press, San Diego
32. Shrout PE, Fleiss JL (1979) Intraclass correlations: uses in assessing rater reliability. Psychol Bull 86:420–428
33. Glass GV, Peckham PD, Sanders JR (1972) Consequences of failure to meet assumptions underlying the fixed effects analysis of variance and covariance. Rev Educ Res 42:237–288
34. Box G (1954) Some theorems on quadratic forms applied in the study of analysis of variance problems, I. Effects of inequality of variance in the one-way classification. Ann Math Stat 25:290–302
35. Souery D, Oswald P, Massat I, Bailer U, Bollen J, Demyttenaere K, Kasper S, Lecrubier Y, Montgomery S, Serretti A, Zohar J, Mendlewicz J, Group for the Study of Resistant Depression (2007) Clinical factors associated with treatment resistance in major depressive disorder: results from a European multicenter study. J Clin Psychiatry 68:1062–1070
36. Lawson RP, Drevets WC, Roiser JP (2013) Defining the habenula in human neuroimaging studies. Neuroimage 64:722–727
37. Geyer S, Weiss M, Reimann K, Lohmann G, Turner R (2011) Microstructural parcellation of the human cerebral cortex—from Brodmann's Post-Mortem Map to in vivo mapping with high-field magnetic resonance imaging. Front Hum Neurosci 5:19
38. Lutti A, Dick F, Sereno MI, Weiskopf N (2014) Using high-resolution quantitative mapping of R1 as an index of cortical myelination. Neuroimage 93:176–188
39. Stüber C, Morawski M, Schäfer A, Labadie C, Wähnert M, Leuze C, Streicher M, Barapatre N, Reimann K, Geyer S, Spemann D, Turner R (2014) Myelin and iron concentration in the human brain: a quantitative study of MRI contrast. Neuroimage 93:95–106
40. Caldwell JD, Shapiro RA, Jirikowski GF, Suleman F (2007) Internalization of sex hormone-binding globulin into neurons and brain cells in vitro and in vivo. Neuroendocrinology 86:84–93
41. Wagner CK, Silverman AJ, Morrell JI (1998) Evidence for estrogen receptor in cell nuclei and axon terminals within the lateral habenula of the rat: regulation during pregnancy. J Comp Neurol 392:330–342
42. Caldwell JD, Höfle S, Englöf I (2002) Sex hormone binding globulin facilitates female sexual receptivity except when coupled to dihydrotestosterone. Brain Res 948:102–107
43. Pawlak J, Brito V, Kuppers E, Beyer C (2005) Regulation of glutamate transporter GLAST and GLT-1 expression in astrocytes by estrogen. Brain Res Mol Brain Res 138:1
44. Auger CJ, Vanzo RJ (2006) Progesterone treatment of adult male rats suppresses arginine vasopressin expression in the bed nucleus of the stria terminalis and the centromedial amygdala. J Neuroendocrinol 18:187–194
45. Spivey JM, Padilla E, Shumake JD, Gonzalez-Lima F (2011) Effects of maternal separation, early handling, and gonadal sex on regional metabolic capacity of the preweanling rat brain. Brain Res 1367:198–206
46. Savitz JB, Rauch SL, Drevets WC (2013) Clinical application of brain imaging for the diagnosis of mood disorders: the current state of play. Mol Psychiatry 18:528–539